Louisiana State University
LSU Digital Commons

Honors Theses | Ogden Honors College

4-2014

On the Amount of Sediment Deposited in Floodplains from the Mississippi River: A Case Study in Cat Island National Wildlife Refuge, Louisiana

Matthew Smith

Follow this and additional works at: https://digitalcommons.lsu.edu/honors_etd

Part of the Geology Commons, and the Geophysics and Seismology Commons

On the Amount of Sediment Deposited in Floodplains from the Mississippi River: A Case Study in Cat Island National Wildlife Refuge, Louisiana

by

Matthew Smith

Undergraduate honors thesis under the direction of

Dr. Samuel Bentley

Department of Geology and Geophysics

Submitted to the LSU Honors College in partial fulfillment of
the Upper Division Honors Program.

April, 2014

Louisiana State University
& Agricultural and Mechanical College
Baton Rouge, Louisiana

Table of Contents

Abstract

To effectively determine sediment available for restoration projects on the Louisiana Coast, it is imperative to know how much sediment the Mississippi River currently provides. One recent study (Allison et al., 2012) demonstrated that between Tarbert Landing and St. Francisville, as much as 50-70 million metric tons (Mt) of sediment per year is lost from river transport, of which ~16 million tons is muddy suspended sediment. Two possible pathways for loss are the storage in the riverbed and the overbank deposition in regions that lack manmade levées. The unlevéed Mississippi east bank near St. Francisville, LA provides the opportunity to investigate the possible pathways of sediment loss. It is relatively undisturbed bottomland forest inundated most years by river flooding. The objective of this study is to determine how much sediment is lost from the river to the Cat Island floodplain, thus gaining an idea of how much sediment could be lost in floodplains along nearby reaches of the river. A total of five 36-50 cm long push-cores were collected in the study area, and then dated by Pb-210 and Cs-137 geochronology methods. Preliminary data suggests that muddy sediment accumulation is equivalent to 1.18-2.25 million tons per year, or 7-14% of muddy suspended sediment lost from river transport.

1. Introduction

For the last 7000-8000 years the Mississippi River has provided sediment to the coast of Louisiana. Throughout this time the river has shifted its course, providing sediment along different localities of the Louisiana coast (Blum and Roberts 2009). This has resulted in a total of six delta lobes (Figure 1) constructed within the last 7000-8000 years. This sediment influx has always combated the natural processes of erosion and subsidence (Allison et al. 2010). Although over the last 7000 years there has been a natural net gain of land, this has changed within the last century.

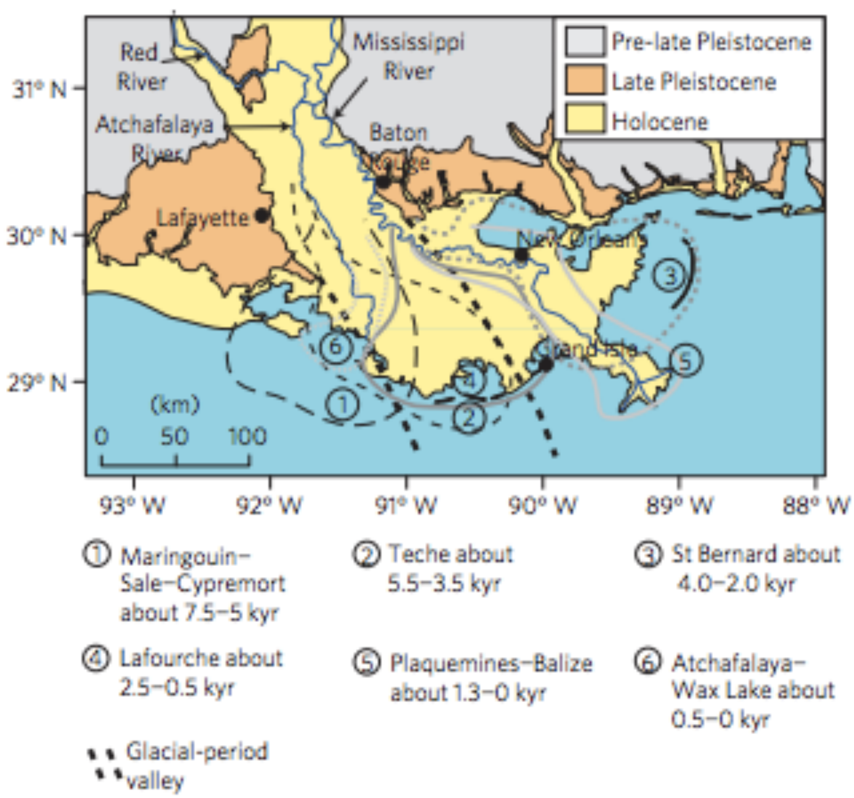

Figure 1: The six Holocene delta lobes formed within the last 7000-8000 years. Currently two delta lobes are being formed/maintained, the Plaquemines-Balize lobe from the Mississippi River, and the Atchafalaya-Wax Lake Delta from the Atchafalaya River. Image from Blum and Roberts 2009.

The change occurred after the 1927 Great Mississippi Flood. The 1927 Great Mississippi Flood was the largest flood in the history of the United States, submerging over 23,000 square miles of land, causing $400 million in damages, and killing 246 people across seven states (John Barry: Rising Tide). After the flood the US Army Corps of Engineers were tasked with creating a system of levées, traps, and dams to help contain the Mississippi River to prevent future catastrophic floods from occurring. This has thus kept the Mississippi River flowing on its current course since 1927, resulting in river sediment not reaching key locations within the delta to combat land loss (Allison et al. 2012). It is predicted that without sediment input 10,000-13,500 km^2 of land will be submerged by the year 2100 (Blum and Roberts 2009). The diversions proposed in the 2012 Master Plan are supposed to mitigate the amount of land being lost. However, for this to be successful we must know how much sediment the Mississippi River can provide.

The data from Allison et al. 2012, as shown in Figure 2, show that 50-70 million metric tons of sediment is lost from transport in-between Tarbert Landing and St. Francisville (Figure 3). It is important for us to know how much sediment is getting trapped within the river and how much is being lost from the system completely from flooding in unlevéed areas of the river. I hypothesize that floodplain sediment storage may account for a significant portion of the "missing" sediment. The coarser sand sediments would deposit along the banks of the river. The amount of sediment that is not lost in these floodplains would be expected to

remain within the river, trapped in areas of low velocity. This study also has implications to hydrology and geomorphology of a large meandering river system.

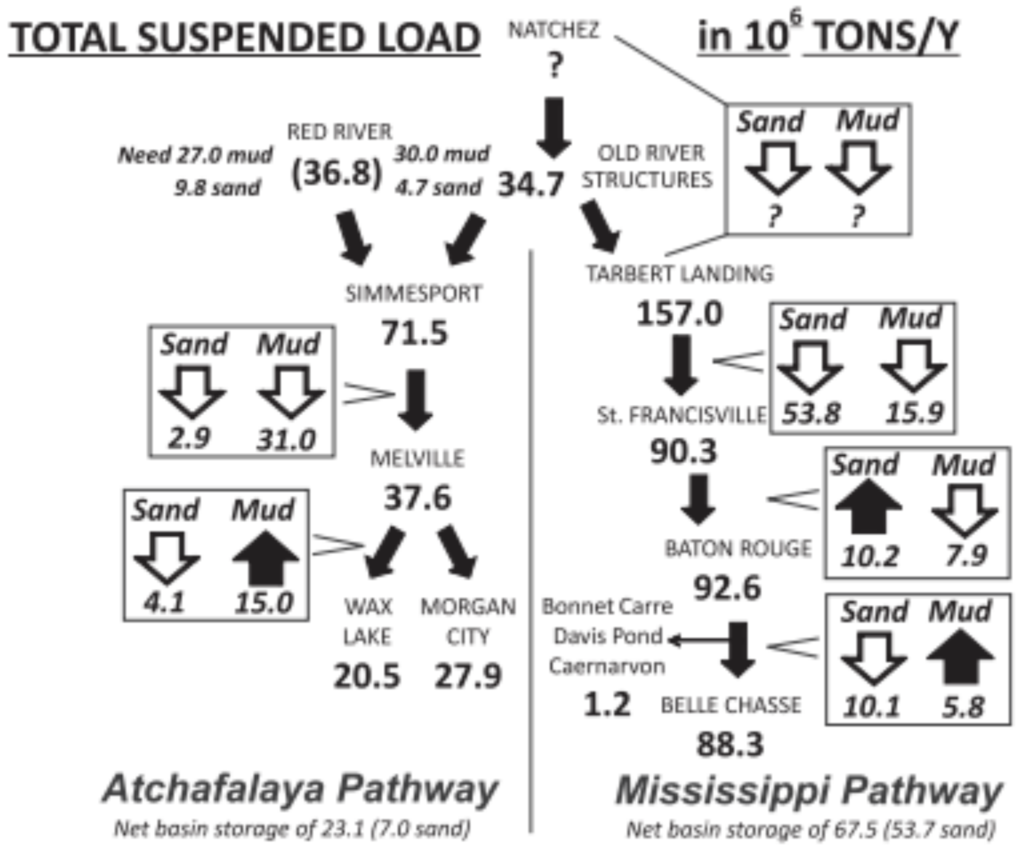

Figure 2: The average total annual discharge in 10^6 tons per year of both the Atchafalaya and Mississippi Rivers. Between Tarbert Landing and St. Francisville the sediment load drops from $157x10^6$ to $90.3x10^6$ per year. This is a decrease of about 50-70 million tons of sediment. Image from Allison et al. 2012.

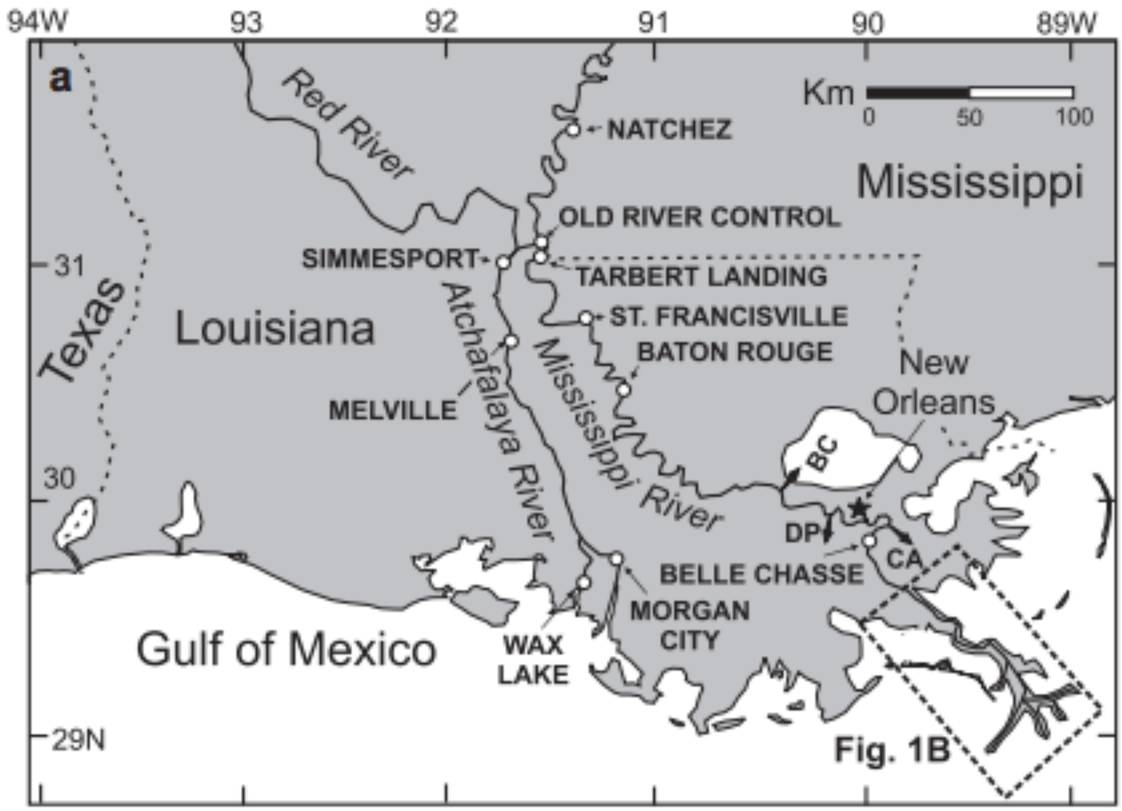

Figure 3: A map showing locations of sediment and water gauging stations along the Mississippi and Atchafalaya Rivers. In between the Tarbert Landing gage and St. Francisville gage 50-70 million tons per year of sediment is either getting trapped within the river, or being deposited in floodplains during flooding events. Image from Allison et al. 2012.

Floodplain sedimentation has been studied worldwide using naturally occurring and anthropogenic radioisotopes as geochronometers. The floodplains of the Rio Beni and Rio Mamore in Bolivia have been thoroughly studied in Aalto et al. (2012), who used Pb-210 to obtain SAR of their cores, however they did not assume an initial concentration of Pb-210 and a constant sedimentation rate, instead they sampled their cores in intervals and at homogenized depths of a few centimeters so that the results yielded excess adsorbed Pb-210 activity profiles that can be

normalized to clay abundance. They did not use Cs-137 due to few locations within the Southern Hemisphere where atmospheric delivery is sufficiently high and variable.

Other similar studies include Aalto et al. (2005) in the Strickland Water system within Papua New Guinea where they used Pb-210 radiochemical data to quantify floodplain sediment accumulation over the last century. There results showed that significant parts of the floodplain have received little to no sediment within the last century, while other areas experienced rapid sediment accumulation. Most of the cores were 80-100 cm approximately double the depth of the cores used in this study. Aalto et al. (2005) did not use Cs-137 to determine SAR. Another difference is that they were only looking for SAR, not MAR.

The Fly River study in Papua New Guinea conducted by Day et al. (2008) found that 40% of the total sediment load was deposited in floodplains. The Fly River study used concentrations of copper within cores to determine SAR, rather than Pb-210. He et al. (1996) uses Pb-210 to determine floodplain depositional rates of the rivers Culm and Exe in Devon, United Kingdoms of the last 100 years. Pb-210 is used over Cs-137 due to it being a "longer-term" radionuclide, since Cs-137 was not introduced until 1954. Results of a small stretch of the floodplain study area were long-term depositional rates of 0.07-0.59 cm/yr.

Goodbred et al. (1998) studied a large heterogeneous part of the Ganges and Brahmaputra river floodplains, using both Cs-137 and Pb-210 to calculate SAR. The point of this study was also to find the correlation between the Cs-137 and Pb-210 results, in which all points showed general good correlation, the greatest difference

being 0.65 cm/yr and >1.0 cm/yr. Within a total area of 36,288 km^2, 167 million tons of sediment per year was deposited within floodplains, approximately 15% of the total discharge that is assumed to reach the ocean.

The Geology of the Cat Island area consists primarily of Quaternary Alluvium due to its close proximity to the Mississippi River. There are also the remnants of older Pleistocene braided-stream deposits, formed during the glacial episodes of the Pleistocene in which the Mississippi River changed from a meandering stream to a braided stream. The result was the formation of Pleistocene terraces that follow alongside the western edge of the Mississippi floodplains (Louisiana Geological Survey, 2008). These flat terraces make it easier for flooding within the western floodplains, compared to the older uplands to the East.

2. Study Area and Methods

The Floodplains of Cat Island National Wildlife Reservation were chosen for this study because of their location between Tarbert Landing and St. Francisville, the area discussed in Allison et al. (2012) that had 50-70 million tons of sediment unaccounted for, it is located 30 miles north of Baton Rouge, and it is a location LSU could obtain permission from which to collect cores. The area is an ideal study location because it is comparatively unaffected by man-made structures, and activities, representing a more natural setting of how sediment loss would be in floodplains. Locations of the Cat Island study area and cores collected are shown in Figures 4 and 5. The total area of unlevéed floodplains was determined using

Google Earth Pro, by creating and measuring areas of polygons within the unlevéed floodplains.

Figure 4: Map showing unlevéed floodplains (yellow polygons) between Tarbert Landing and Baton Rouge.

Figure 5: Zoomed in view of the black box in Figure 4 showing the five core locations taken in Cat Island National Reserve.

2.1 Collection

On September 2, 2013, four pushcores were collected from Cat Island National Wildlife Reserve (Figure 5) with penetration depths of 36-47 centimeters for the purpose of radiochemical analysis of Pb-210, Cs-137, and granulometry. A 50 cm preliminary core was also collected on February 11, 2014. Cores at differing distances from the river were desired. The core locations were influenced by where the survey team was able to travel to, using a path and carrying the core collection gear. The cores were collected using a 2 1/2” x 40” Gouge Auger (Figure 7). After the cores were excavated from the ground and measured, they were covered with plastic wrap and then removed from the pipe using bent cake icing spreaders and placed within a PVC pipe that was split longitudinally. After marking the top part of the core, the other half of the PVC pipe was then placed on top and taped closed, using parts of Styrofoam pool noodles to plug the ends of the core, ensuring it did not shift in transit. A field picture of a core being processed can be seen in Figure 6. In the lab the cores were cut in half vertically, with half being used for radiochemistry data and the other half being used for image spectrometry and grain size analysis.

Figure 6: Edward Lo (left) and Matthew Smith (right) record and process a core from Cat Island.

Image provided by Dr. Bentley.

Figure 7: The 2 1/2" x 40" Gouge Auger used to collect the cores in Cat Island.

2.2 Radiochemistry

To estimate the sedimentation rates and mass accumulation rates (MAR) within these unlevéed floodplains, radiochemical data for Pb-210 and Cs-137 activities were obtained. Pb-210 is a naturally occurring radionuclide obtained from the atmosphere and Cs-137 is from the nuclear fallout from hydrogen bomb testing during the 1960's. Pb-210 is part of the U-238 decay series and has been commonly used to determine sedimentary processes on centennial timescales. Pb-210 has a half-life of 22.3 years, and a decay constant of 0.031 yr^{-1}. It is produced in the atmosphere from the decay of Rn-222 and within sediments and bedrock (Hulse and Bentley 2012). Radiochemical data were obtained using the method of Bentley (2014). The samples for radiochemical analysis were cut into 2 cm increments, dried, ground, and sealed in 50x9 mm petri dishes. They were then measured on low-background planar gamma detectors for 24 hours. The sedimentation accumulation rate (SAR) of Pb-210 was calculated from:

$$A_z = A_0 e^{(-\lambda z/S)} \qquad \text{Equation 1}$$

where A_0 is the Pb-210 activity decay per minute per gram (dpm/g) at the surface, A_z is the Pb-210 activity (dpm/g) at depth z (cm), λ (yr^{-1}) is the decay constant, which is 0.031 yr^{-1}, and S (cm/yr) is the SAR (Hulse and Bentley 2012). The SAR of Cs-137 from:

$$S = (z_{max} - L_b)/(T-1954) \qquad \text{Equation 2}$$

where S is the SAR, z_{max} is the maximum depth that Cs-137 is observable, L_b is the bioturbation rate (for this study the bioturbation rate was assumed to be zero), and

T is the year in which the cores were collected. The Mass Accumulation Rate (MAR) is calculated from:

$$S*(P_s*(1-\phi))=MAR \qquad \text{Equation 3}$$

in which S=sedimentation rate, P_s=grain density, estimated at 2.65 g/cm^3, and ϕ=porosity, estimated at 0.6.

2.3 Grain Size

Samples were then homogenized, and 5-10g of sediment was taken and placed in a centrifuge tube. A sodium phosphate solution of 0.05% was then added to break up the sediment into individual grains. The samples were then shaken and allowed to sit for 2-3 days, being shaken up once a day. Once the sediment becomes separated into individual grains it was run through a 2 mm sieve to remove any organics, such as roots or leaves that are in the sample. The sample was then run through a Beckman-Coulter LS 13-320 laser diffraction instrument on range of 0.375124-1821.88 um to determine the grain sizes of the cores (Hulse and Bentley, 2012).

2.4 Color Imaging

Color Imaging was conducted on core 9.2.13-4 due to its completeness post extraction. 9.2.13-4 was wetter than the other cores, and so it remained continuous while the other cores were drier and broke in places during extraction. This is likely due to the higher clay content that 9.2.13-1 and 9.2.13-4 have over 9.2.13-2 and 9.2.13-3, allowing for the core to retain water and stick together better, and 9.2.13-4

likely remained more wet compared to core 9.2.13-1 due to its closer proximity to the river and thus exposed to water more frequently. The image of 9.2.13-4 can be seen in Figure 8.

Figure 8: Color image of core 9.2.13-4. Grains are primarily silt and clay with some sand grains most common at the top of the core. Some roots and leaves included in the top of the core. Length of core is 46 cm, width is 6 cm.

3. Results

Application of Equations 1 and 2 to radionuclide data yields the following SARs. Cs-137 and Pb-210 data from core 9.2.13-1 indicate a sediment accumulation rate of 0.18-0.22 cm/yr and 0.41 cm/yr respectively (Figure 9). For 9.2.13-2 Cs-137 shows >0.59 cm/yr and Pb-210 shows 1.5 cm/yr (Figure 10). 9.2.13-3 Cs-137 shows >0.59 cm/yr and Pb-210 shows 0.56 cm/yr (Figure 11). 9.2.13-4 Cs-137 shows 0.50 cm/yr and Pb-210 shows 0.28 cm/yr (Figure 12). Equation 3 was used to determine MAR from each SAR, averaged for Pb-210 and Cs-137 for each core. The average is used because there is not a way to distinguish which SAR is more accurate, and the range of Pb-210 and Cs-137 SARs likely represents the range of uncertainty for the measurements. The MAR for 9.2.13-1 is 0.32 g/cm^2 per year. MAR of 9.2.13-2 is 1.11 g/cm^2 per year. MAR of 9.2.13-3 is 0.61 g/cm^2 per year. MAR of 9.2.13-4 is 0.41 g/cm^2 per year. Core CI-1A, collected from the natural levee of the river north of the Cat Island NWR, contains trace amounts of Cs-137 to a depth of 46 cm, suggesting that at least the upper ~46 cm have been deposited since 1954. Pb-210 activity shows no obvious decline with depth, suggesting that the entire core has been deposited during time period less than the half life of Pb-210, or ~22 years. These observations allow calculation of minimum SAR for this core using Cs-137 of >0.75 cm/yr, and for Pb-210, >2.2 cm/yr (Figure 13).

	Cs-137 SAR (cm/yr)	Pb-210 SAR (cm/yr)	Averaged MAR (g/cm^2/year)
9.2.13-1	0.18-0.22	0.41	0.32
9.2.13-2	>0.59	1.5	1.11
9.2.13-3	>0.59	0.56	0.61
9.2.13-4	0.50	0.28	0.41
CI-1A	>0.75	>2.2	1.56

Table 1: Displays for each core the average sediment accumulation rate (SAR) of both Cs-137 and Pb-210 and the mass accumulation rate (MAR) of the core.

Results of grain size data can be seen in Figures 7-10. Grains that are <3.9 um are clay, 3.9-63 um are silt, and >63 um are sand. The dominating grain size in all of the cores from the floodplain away from natural levées was silt. At the top of cores there was a higher concentration of sand than clay, but deeper in the core clay was a higher concentration than sand. Cores 9.2.13-1 and 9.2.13-4 have larger differences in concentration between the sand and clay particles than 9.2.13-2 and 9.2.13-3, with clay particles being the dominant form.

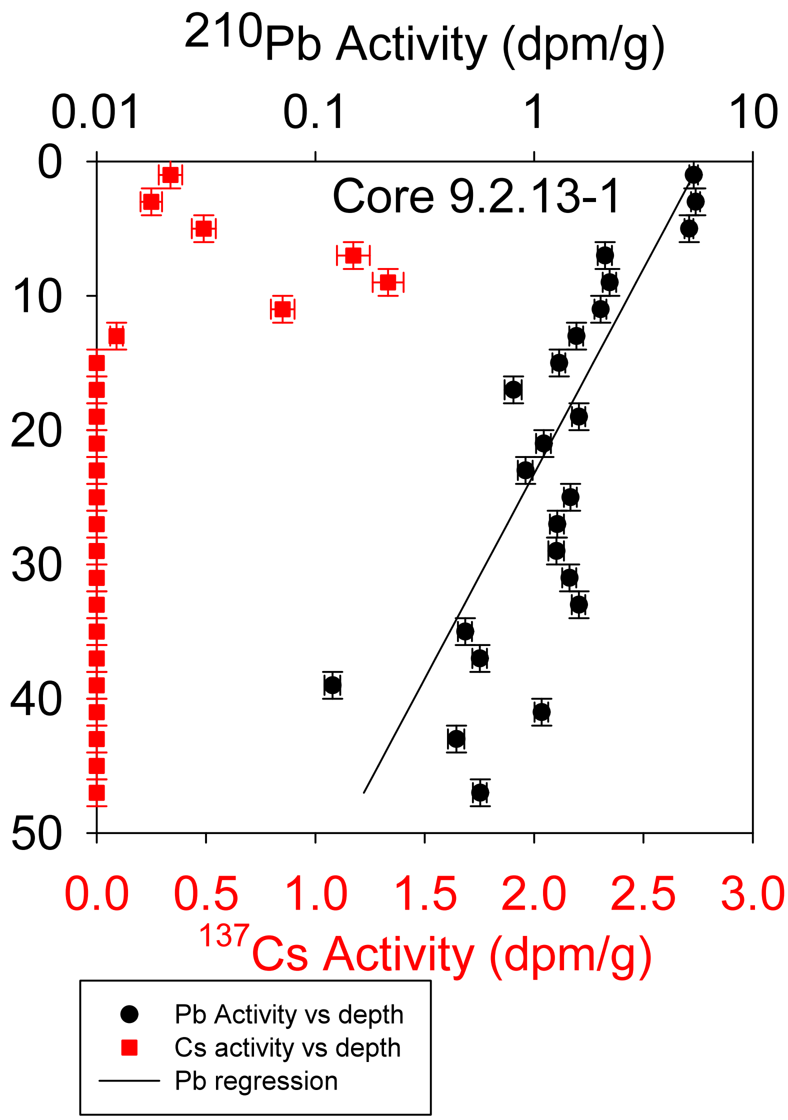

Figure 9: Pb-210 and Cs-137 Profile of Core 9.2.13-1. Cs-137 and Pb-210 data indicate a sedimentation rate of 0.18-0.22 cm/yr and 0.41 cm/yr respectively.

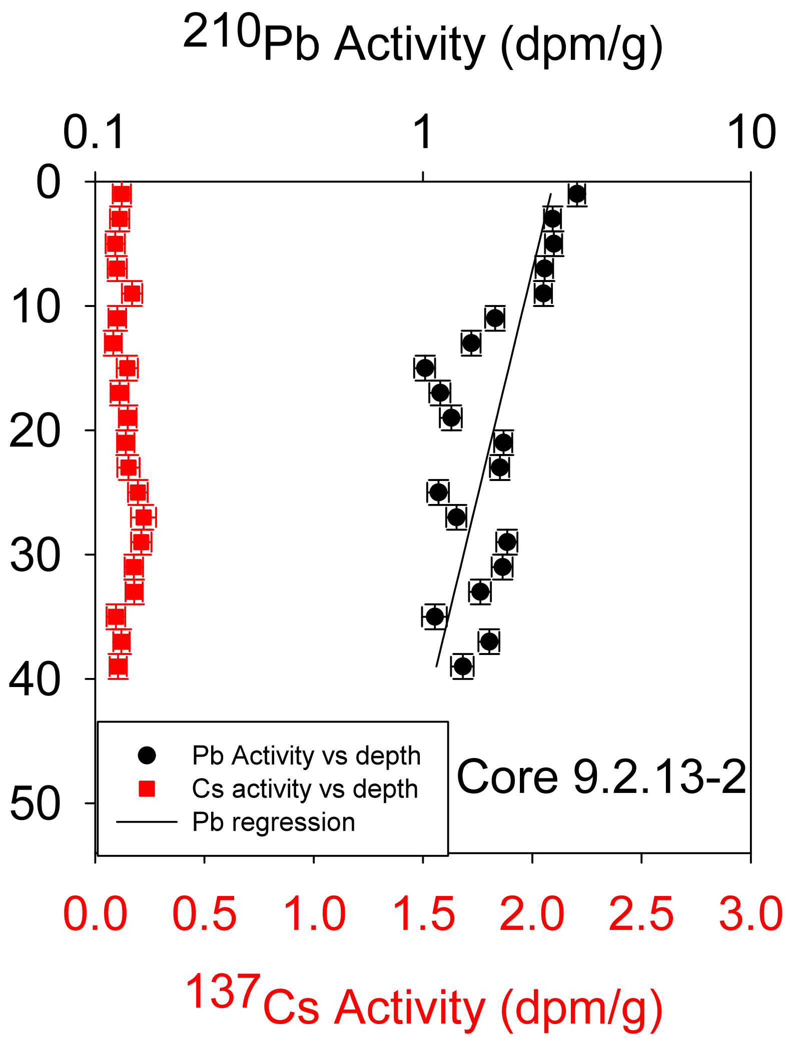

Figure 10: Pb-210 and Cs-137 Profile of Core 9.2.13-2. Cs-137 and Pb-210 data indicate a sedimentation rate of >0.59 cm/yr and 1.5 cm/yr respectively.

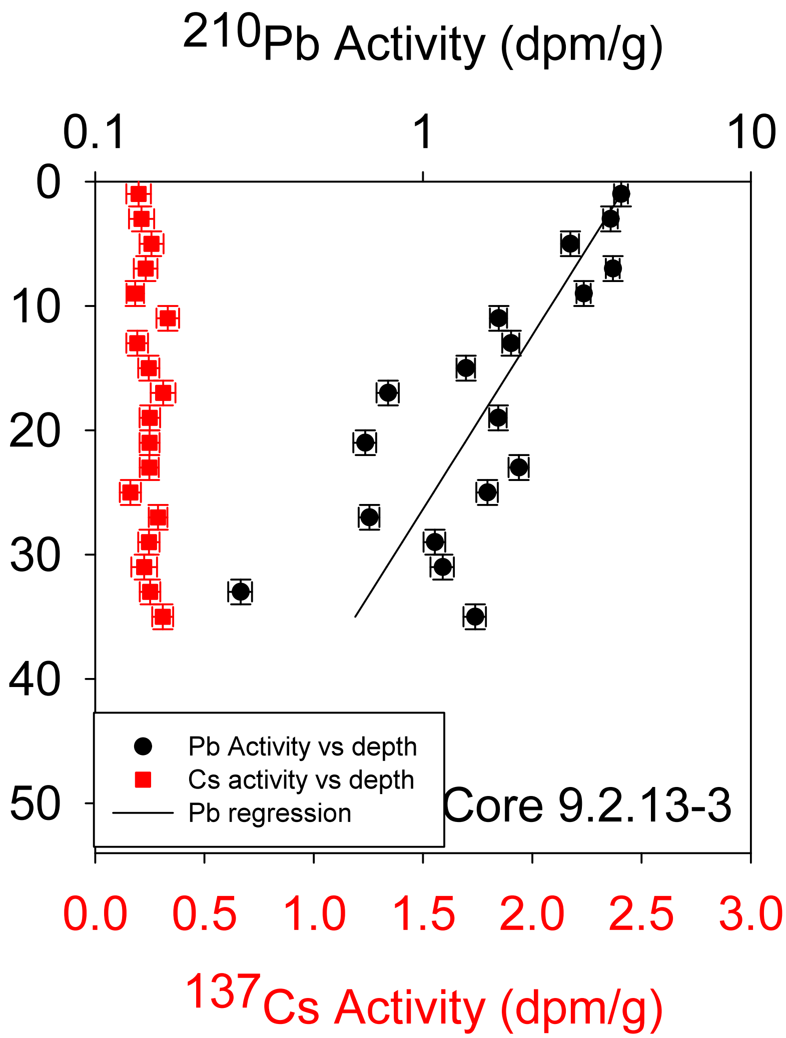

Figure 11: Pb-210 and Cs-137 Profile of Core 9.2.13-3. Cs-137 and Pb-210 data indicate a sedimentation rate of >0.59 cm/yr and 0.56 cm/yr respectively.

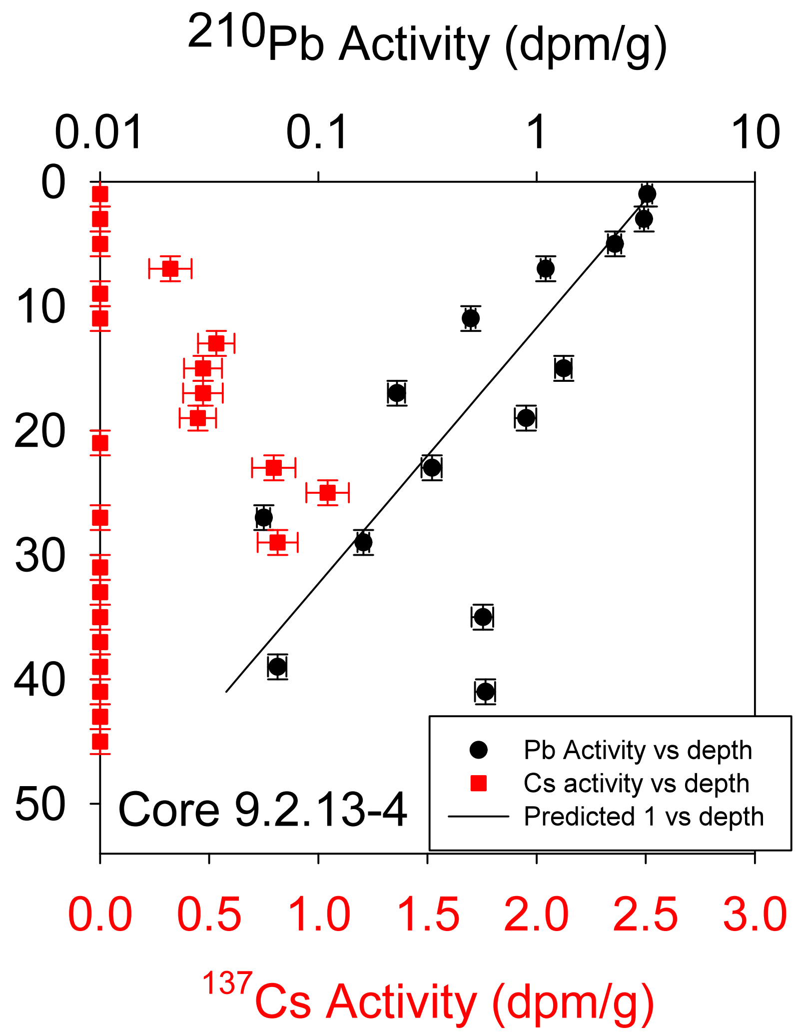

Figure 12: Pb-210 and Cs-137 Profile of Core 9.2.13-4. Cs-137 and Pb-210 data indicate a sedimentation rate of 0.50 cm/yr and 0.28 cm/yr respectively.

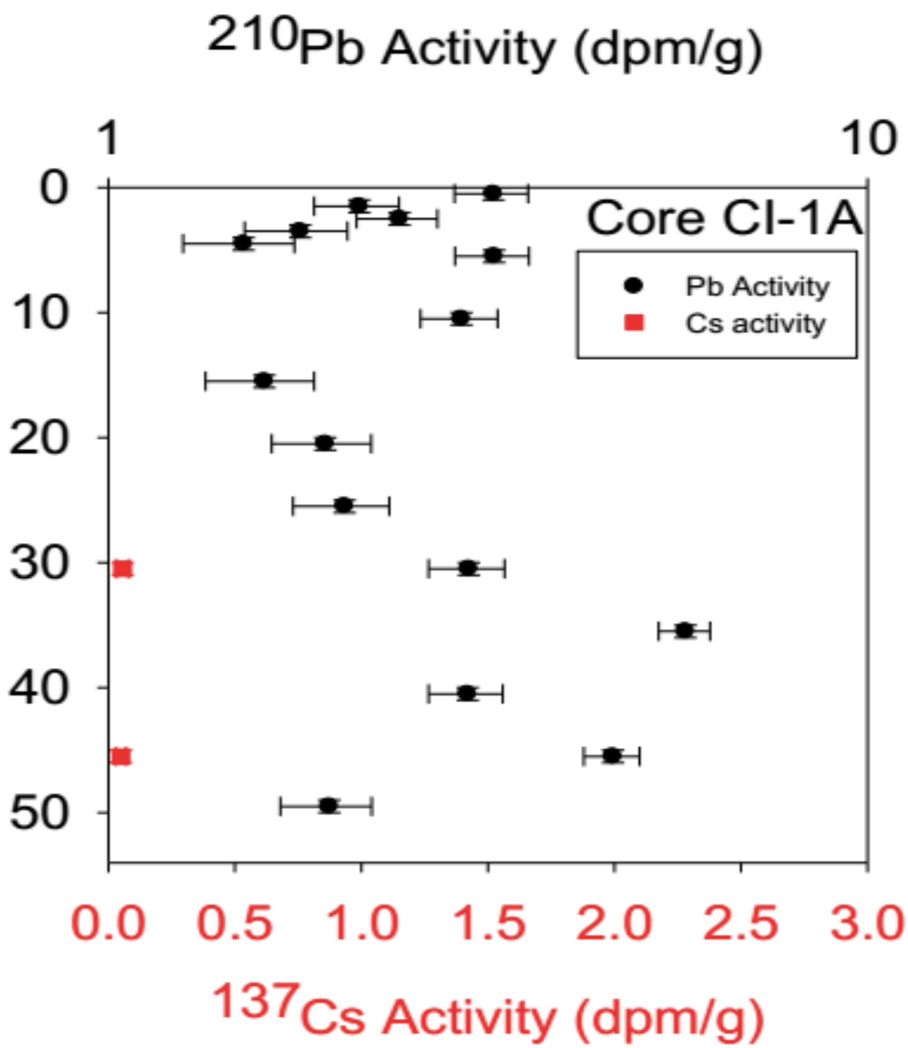

Figure 13: Pb-210 and Cs-137 Profile of Core CI-1A. Cs-137 and Pb-210 data indicate a sedimentation rate of >0.75 cm/yr and >2.2 cm/yr respectively.

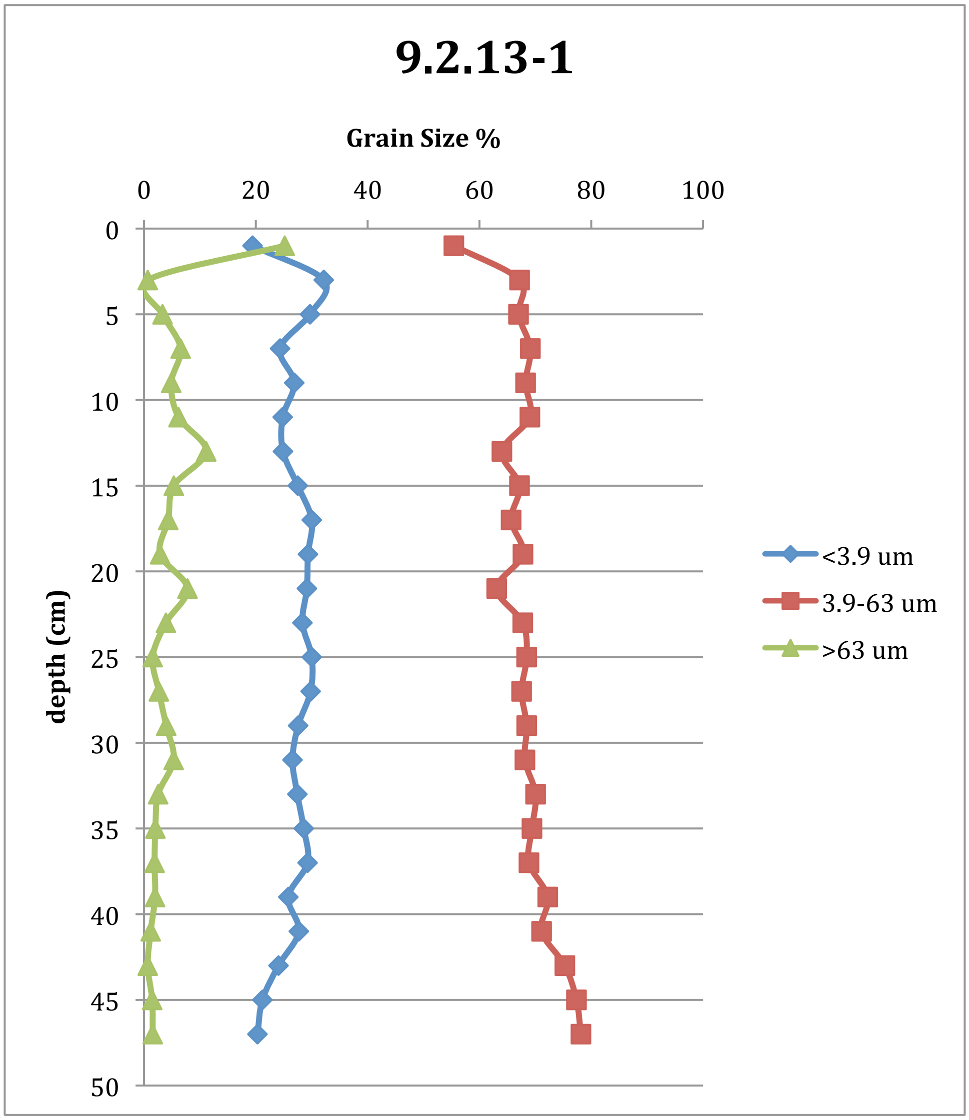

Figure 14: Grain size data of core 9.2.13-1. Dominated by silt, with sand being more than clay at the very top of the core, but in small concentrations after this. Length of core was 47 cm.

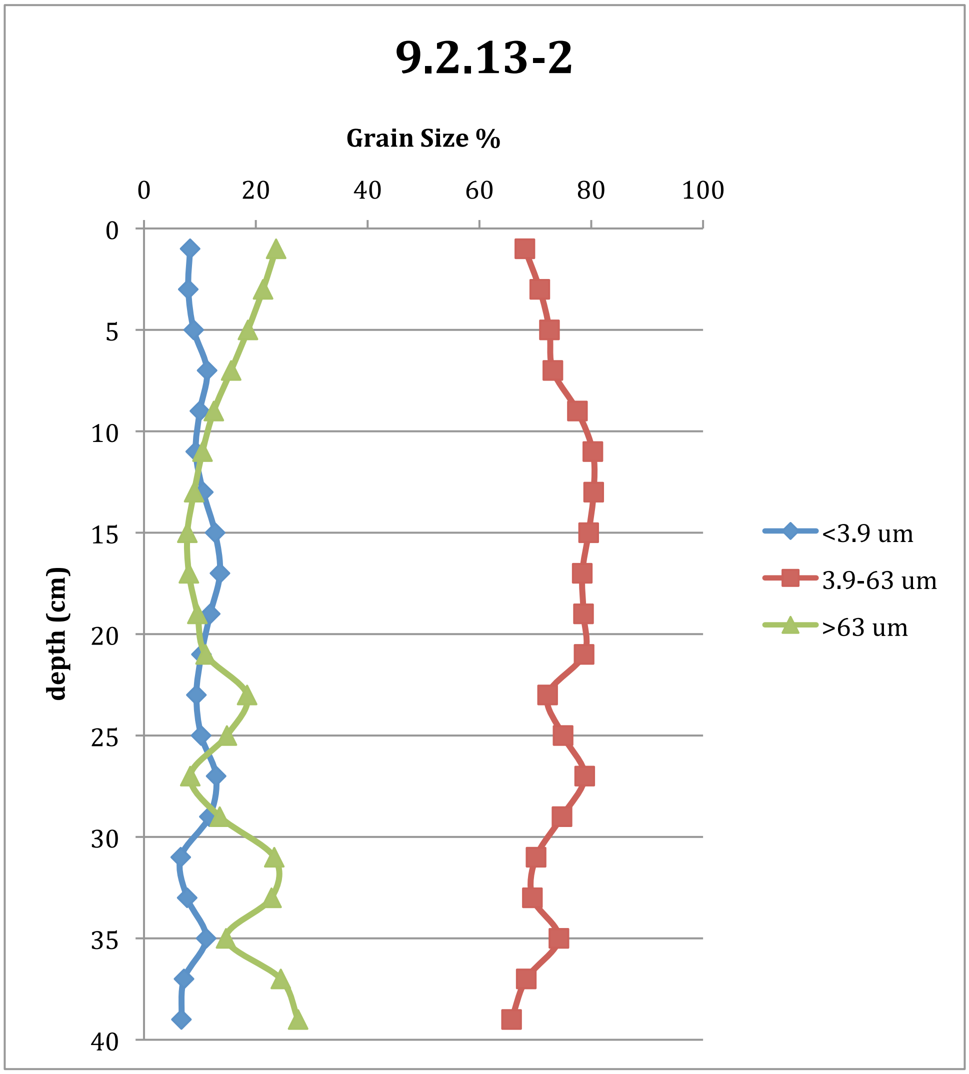

Figure 15: Grain size data of core 9.2.13-2. Mostly contains silt. Sand and clay particles have similar concentrations throughout the core. Length of core was 40 cm.

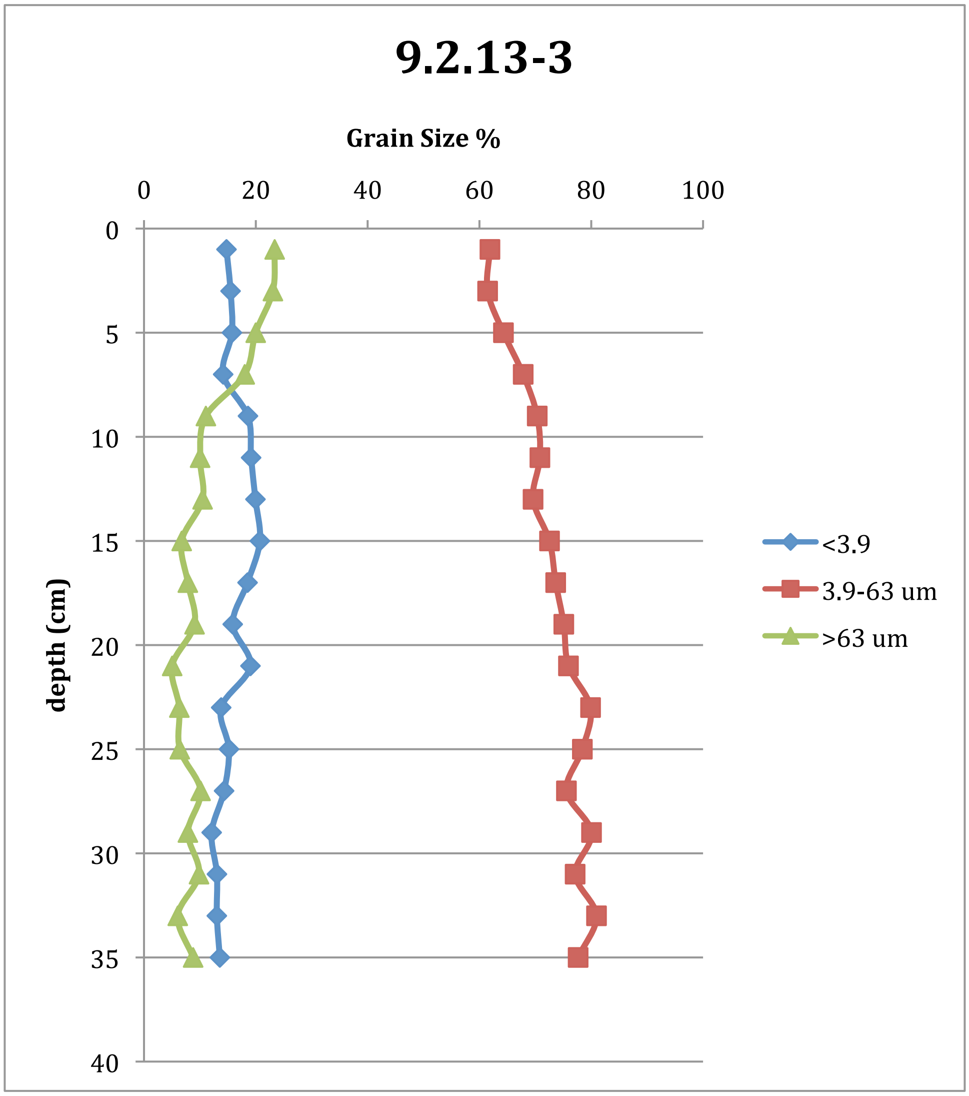

Figure 16: Grain size data of core 9.2.13-3. Dominated by silt. At the top of the core there is more sand than clay, but this changes about 9 cm deep. Length of core was 36 cm.

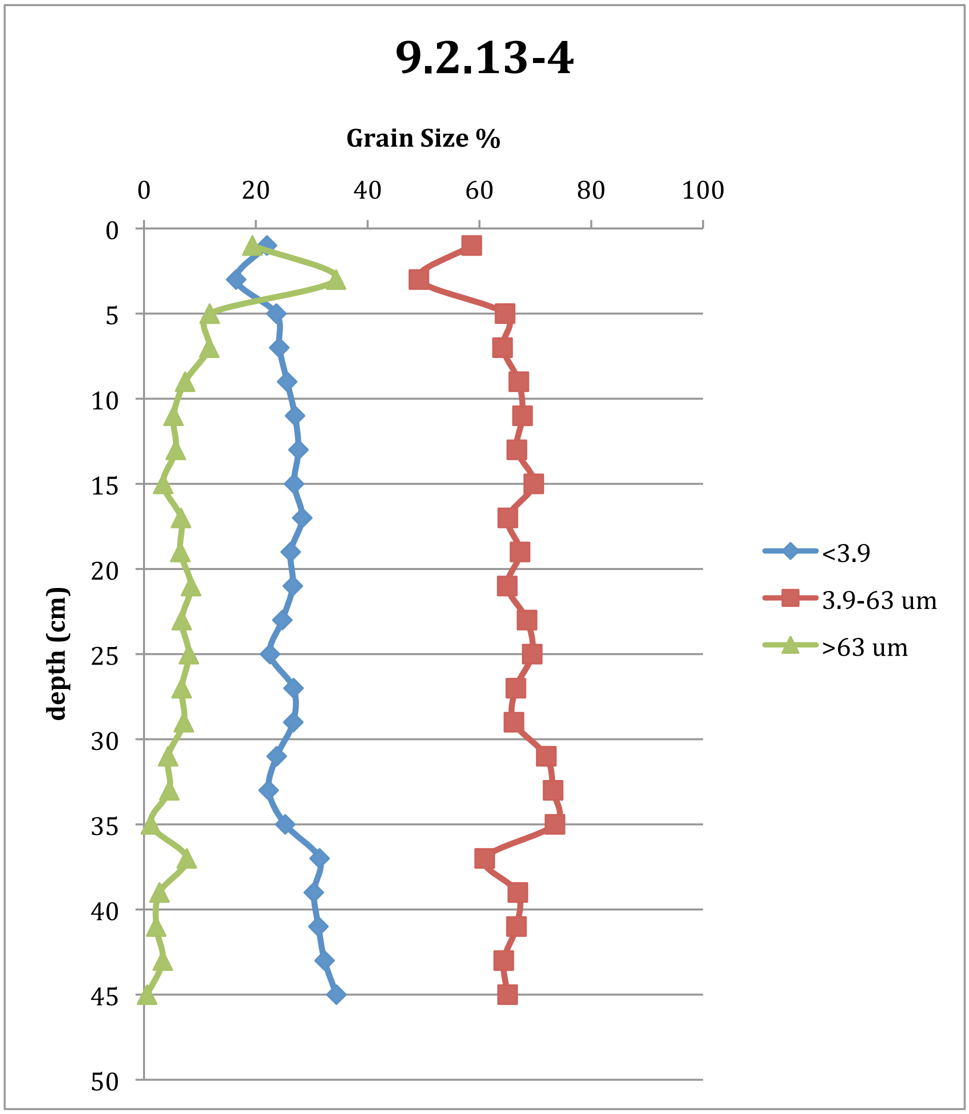

Figure 17: Grain size data of core 9.2.13-4. Mostly contains silt. There is higher sand concentration than clay at 3 cm in the core, but higher clay concentration throughout the rest of the core. Length of core was 46 cm.

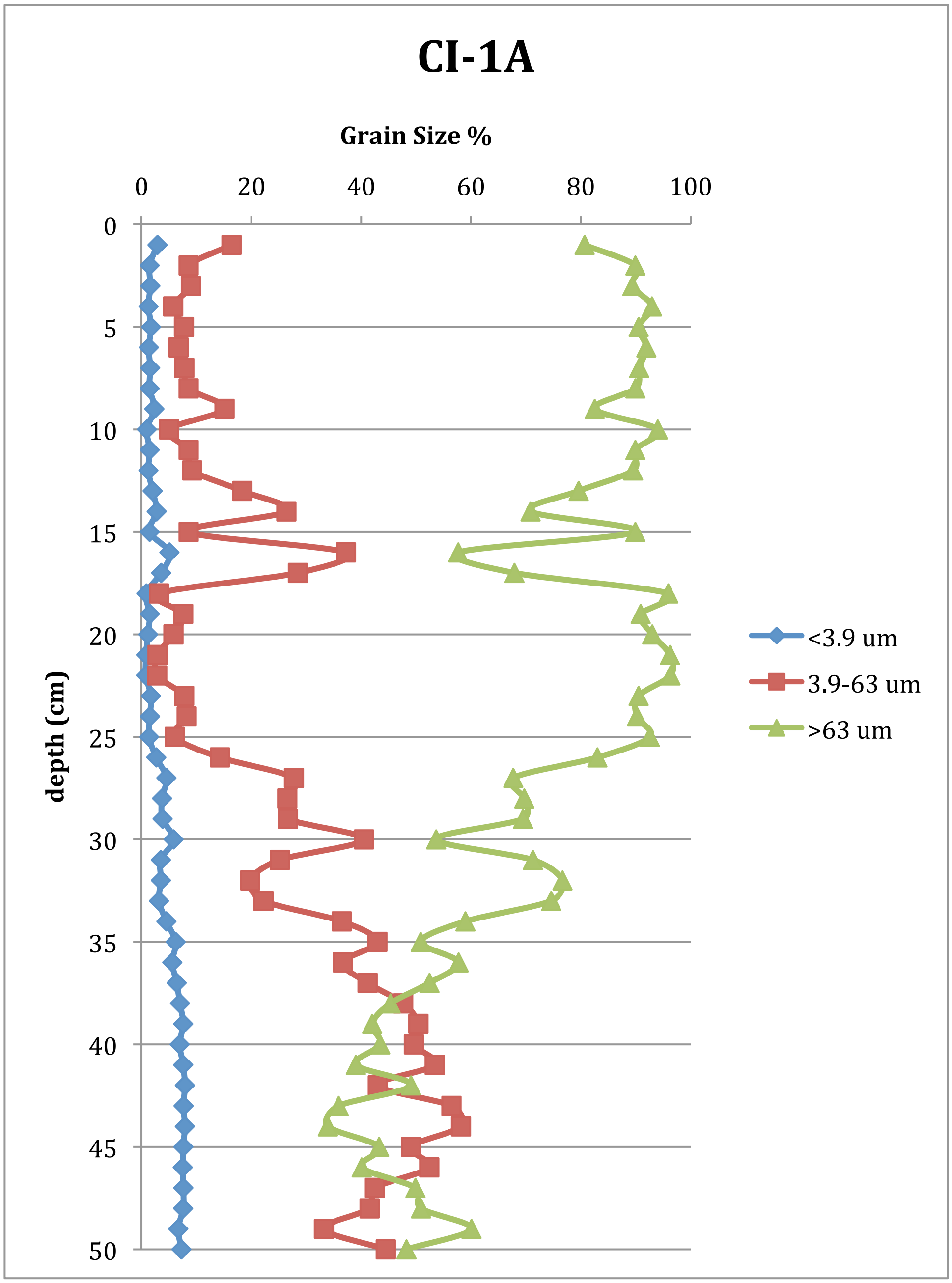

Figure 18: Grain size data of core CI-1A. Mostly comprised of sand. There is higher silt concentration than clay. From 30-50 cm silt and sand evenly comprise ~40-45% of the core. Length of core was 50 cm.

4. Discussion

Cs-137 spikes are observable in cores 9.2.13-1 and 9.2.13-4, Figures 11 and 14 respectively. The first appearance of Cs-137 would be 1954, and the peak of Cs-137 would be 1963, when hydrogen bomb testing was the greatest (Irlweck et al. 1985). There is not an observable peak in cores 9.2.13-2 and 9.2.13-3 as seen in Figures 12 and 13 respectively. The SAR of >0.59 cm/yr is a minimum SAR, since we know the sediment in these cores are younger than 1954, since Cs-137 is present to the core base. The explanation for not having a Cs-137 spike is the combination of the 9.2.13-2 and 9.2.13-3 cores being shorter than the other cores and both having a higher sedimentation rate. Thus the 1963 peak would have been located further down than in the cores with slower sedimentation rates and would not appear within the 40 cm and 36 cm cores. An issue with this is that we do not know exactly how much deeper we would have to go to see the 1963 Cs-137 spike, and would need to collect deeper cores to resolve this issue. Also what can be observed is that the Cs-137 concentration is decreasing. Without a new source, it will eventually not appear in the system at all, and while the 1963 marker can be useful if a deep enough core is obtained, it will soon become less and less accurate towards finding the sedimentation rate of a region (Aalto et al. 2012).

The Pb-210 values obtained for muddy floodplain cores are within a similar range, with the exception of core 9.2.13-2, which had a sedimentation rate of 1.5 cm/yr. The cause of this anomaly is inconclusive, however a possible explanation is that the spot that 9.2.13-2 was collected at was at a slightly lower topographic level than 9.2.13-3, allowing for more sediment to be deposited. Regardless, some sort of

mechanism must have been involved to allow for more efficient deposition of sediment at 9.2.13-2, which can be studied in the future. As seen in Figure 9, Pb-210 data for core 9.2.13-1 show activities of Pb-210 are nearly constant over approximately six centimeters or more. These sections likely indicate periods when a large amount of sediment was deposited at once, such as large flooding events. Taking the sedimentation rate and dividing by the depth within the core can provide us with the approximate year that section was deposited in. The grouping at the 30 cm depth correlates to about 1927, indicating that the 1927 Great Flood likely caused the grouping of Pb-210 points. The grouping of data points at the top of the core can be attributed to the 2011 flood. Thus the 2011 flood deposited as much as the top 6 cm of the core.

The grain sizes of all the cores remain largely consistent with silt, ranging from 3.9-63 um, being the dominant grain size between 60-80% of the entire core. Cores 9.2.13-1 and 9.2.13-4 have a larger difference between the sand and clay particles than 9.2.13-2 and 9.2.13-3 because 9.2.13-1 and 9.2.13-4 are located further away from the source, the Mississippi River, and would not receive as much sand grains, since they would be deposited before the silt and clay particles. The amount of silt was typically the smallest at the top, likely due to recent flooding that would allow for sand particles to have a higher percentage before bioturbation could homogenize the sediment. Clay, <3.9 um, was usually the second most dominant grain size, being overtaken by sand, >63 um, at the top of the core as seen by cores 9.2.13-1, 9.2.13-3, and 9.2.13-4. Core 9.2.13-2 for the majority of the core had more sand than clay grains. This is due to its close proximity to the river and

because of its high SAR as shown by its Pb-210 data. A higher SAR would indicate more water flowing through the area than the other cores, allowing for a larger amount of sand to be deposited. Core 9.2.13-1 has the overall lowest concentration of sand due to it being located furthest from the river, and thus most of the sand would have been deposited before reaching 9.2.13-1. The fine sediment of the cores is indicative of similar energy during flooding events, but also likely due to the proximity of the cores being far enough from the river for larger grains to have deposited before reaching the core sites. Grain size for core CI-1A is much coarser than for other cores, consistent with its location <200m from the riverbank. The coarse grain size might account for low and variable activities of Cs-137 and Pb-210, which generally adhere better to clay and silt sized grains than to sand (Krishnaswami and Cochran, 2008).

Our study area of Cat Island is approximately 139 km^2. The MAR for all of the cores have a range from 0.32 to 0.61 g/cm^2 per year, or 3200-6100 metric tons per km^2 per year (with the exception of 9.2.13-2 due to its extremely high Pb-210 sedimentation rate). 9.2.13-1 has the lowest MAR, which seems logical due to it being furthest from the river. However, it is also close to a bayou that could be a conduit for sediment transport away from the river during flooding. The large sediment accumulation rate from Pb-210 of 9.2.13-2 is anomalously high compared to the other cores, and is not used for additional calculations until we can better explain these results.

The total unlevéed area of the Cat Island floodplain (Figure 4) is ~139 km^2. The Raccourci Island floodplain and lake area constitute an additional ~137 km^2,

with an additional 94 km^2 of unlevéed floodplain between Cat Island and Baton Rouge. Using the total area of Raccourci Island and Cat Island (276 km^2) and the range of MARs above, this suggests that 1.64-2.11 million tons per year of muddy sediment are probably accumulating in the unlevéed floodplains between Tarbert Landing and Cat Island, with an extra 0.56-0.72 million tons per year of muddy sediment between St. Francisville and Baton Rouge (94 km^2). This amount is equal to 7-14% of the muddy sediment lost between Tarbert Landing and St. Francisville, a distance of about 33.37 km, as determined by Allison et al. (2012). This depositional rate is likely close to the average depositional rate along the stretch between Tarbert Landing and St. Francisville since it is located along a straight part of the river, most of this section is straight, with three total bends, only one of them being particularly sharp. SAR would be expected to be slightly greater along the outer bank of bends due to increased velocity of the river and likely higher concentrations of sediment entering the floodplain. Abundant fresh sand deposits were also observed on natural levées adjacent the river, but were not quantified for this study. Locations of the river that have a decrease in water discharge and velocity would allow for sediment to be deposited along the riverbed. The amount of sediment deposited within a certain area of the river could be calculated by using the MAR equation, with MAR being a known value, and SAR being the unknown. This study can loosely be applied to other areas of the Mississippi River since it is part of the same river system. However other river systems will have a unique amount of river discharge, periods of flooding, and sediment budget that would

make it difficult to generalize the results from this study and apply them to these other river systems.

5. Conclusion

Sediment deposition in unlevéed floodplains is just one pathway for the loss of transported sediment. Assuming similar deposition rates as seen in this study, 1.64-2.11 millions tons of sediment is being deposited per year within unlevéed floodplains between Tarbert Landing and St. Francisville. This however only attributes to a small percentage of the total "missing" sediment from the Allison et al. 2012 study. Thus another sediment sink must be identified to account for this other sediment. Assuming the rest of the "missing" sediment is being deposited within sections of the Mississippi River, this could lead to accretion of the riverbed. This would lead to the river height increasing, which could lead to the river flooding over the levées. Thus these sections may require dredging to ensure the river does not overflow the levée system.

6. Future Work

This study provides insights into transport, storage, and loss of sediment from the Mississippi River. Such information is vital for determining feasibility of coastal restoration programs that may be sediment limited. More of the unlevéed areas between the Old River Control Structure and Baton Rouge should be studied to compare the rate of sediment deposition to achieve a more complete understanding of the sediment available for restoration projects. More studies are

needed to investigate the causes of sedimentation rates beyond just distance from the river. Deeper cores should be obtained in the future in an attempt to include the Cs-137 peak, or the 1963 indicator, in all cores. Attempting to include bioturbation rates into the calculation of SAR would provide more accurate SAR results.

7. Acknowledgements

I would like to thank Dr. Peter Clift, Crawford White, Tara Jonell, Gregory Keller, and Edward Lo for field assistance at Cat Island, and Jillian Banks, Kathryn Denommee, Crawford White, and James Smith for assistance within the lab. Funding was provided by the College of Science, the Honors College, and the Billy and Ann Harrison Endowment for Sedimentary Geology, with the LSU Foundation. Finally I would like to thank my committee members Dr. Kehui Xu, Dr. Tiffany Roberts, and my advisor Dr. Samuel Bentley.

8. References

Aalto, R. and Dietrich, W., (2005) "Sediment accumulation determined with ^{210}Pb geochronology for Strickland River flood plains, Papua New Guinea." *Sediment Budgets I (2005) 291.*

Aalto, R. and Nittrouer, C., (2012) "210Pb geochronology of flood events in large tropical river systems." *Phil. Trans. R. Soc. A (2012) 370, 2040–2074*. DOI: 10.1098/rsta.2011.0607

Allison, Mead A., and Ehab A. Meselhe, (2010) "The Use of Large Water and Sediment Diversions in the Lower Mississippi River (Louisiana) for Coastal Restoration." *Journal of Hydrology 387.2010: 346-60. Web.*

Allison, Mead A., C. R. Demas, B. A. Ebersole, B. A. Kleiss, C. D. Little, E. A. Meselhe, N. J. Powell, T. C. Pratt, B. M. Vosburg, (2012) "A water and sediment budget for the lower Mississippi–Atchafalaya River in flood years 2008–2010: Implications for sediment discharge to the oceans and coastal restoration in Louisiana." *Journal of Hydrology 432-433.2012: 84-97. Web.*

Barry, John M. *Rising Tide: The Great Mississippi Flood of 1927 and How It Changed America*. New York: Simon & Schuster, 1997. Print.

Bentley, Sr., S.J., et al., *Sedimentation, bioturbation, and sedimentary fabric evolution on a modern mesotidal mudflat: A multi-tracer study of processes, rates, and scales*, Estuarine, Coastal and Shelf Science (2014), http://dx.doi.org/10.1016/j.ecss.2014.02.004

Blum, Michael D., and Harry H. Roberts. (2009) "Drowning of the Mississippi Delta Due to Insufficient Sediment Supply and Global Sea-level Rise." *Nature Geoscience 2: 488-91. Web.*

Coastal Protection and Restoration Authority of Louisiana. 2012. *Louisiana's Comprehensive Master Plan for a Sustainable Coast*. Coastal Protection and Restoration Authority of Louisiana. Baton Rouge, LA.

Day, G., W. E. Dietrich, J. C. Rowland, and A. Marshall, (2008) "The depositional web on the floodplain of the Fly River, Papua New Guinea." *J. Geophys.* Res., 113, F01S02, doi:10.1029/2006JF000622.

Louisiana Geological Survey, (2008) "Generalized Geology of Louisiana." Web. 5 Apr. 2014. <http://www.lgs.lsu.edu/deploy/uploads/gengeotext.pdf>.

Goodbred, S. L., Jr & Kuehl, S. A., (1998) "Floodplain processes in the Bengal Basin and the storage of Ganges-Brahmaputra river sediment: an accretion study using Cs-137 and Pb-210 geochronology." *Sedimentary Geology* **121**, 239-258.

He, Q. and Walling, D. E., (1996) "USE OF FALLOUT Pb-210 MEASUREMENTS TO INVESTIGATE LONGER-TERM RATES AND PATTERNS OF OVERBANK SEDIMENT DEPOSITION ON THE FLOODPLAINS OF LOWLAND RIVERS." *Earth Surface Processes and Landforms*, 21: 141–154. doi: 10.1002/(SICI)1096- 9837(199602)21:2<141::AID-ESP572>3.0.CO;2-9

Hulse, P. and Bentley, S., (2012) “A ^{210}Pb sediment budget and granulometric record of sediment fluxes in a subarctic deltaic system: The Great Whale River, Canada.” *Estuarine, Coastal and Shelf Science* **109**, 41-52.

Irlweck, K. and Danielopol, D. L., (1985) “Caesium-137 and lead-210 dating of recent sediments from Mondsee (Austria).” *Hydrobiologia* **128**, Issue 2, pp 175-185. doi:10.1007/BF00008737.

Krishnaswami, S., and Cochran, J.K., (2008) “U-Th series nuclides in aquatic systems.” *Radioactivity in the Environment*, v. 13. Elsevier (Amsterdam), p. 458